Food Chemistry 188 (2015) 161–169

Contents lists available at ScienceDirect

Food Chemistry

journal homepage: www.elsevier.com/locate/foodchem

# Adsorption of nisin and pediocin on nanoclays

Stela Maris Meister Meira, Arthur Izé Jardim, Adriano Brandelli *

*Laboratório de Bioquímica e Microbiologia Aplicada, Instituto de Ciência e Tecnologia de Alimentos (ICTA), Universidade Federal do Rio Grande do Sul (UFRGS), 91501-970 Porto Alegre, RS, Brazil*

ARTICLE INFO

*Article history:*
Received 2 September 2014
Received in revised form 3 April 2015
Accepted 29 April 2015
Available online 29 April 2015

*Keywords:*
Bacteriocin
Adsorption
Nanoclay
Halloysite
Montmorillonite

ABSTRACT

Three different nanoclays (bentonite, octadecylamine-modified montmorillonite and halloysite) were studied as potential carriers for the antimicrobial peptides nisin and pediocin. Adsorption occurred from peptide solutions in contact with nanoclays at room temperature. Higher adsorption of nisin and pediocin was obtained on bentonite. The antimicrobial activity of the resultant bacteriocin-nanoclay systems was analyzed using skimmed milk agar as food simulant and the largest inhibition zones were observed against Gram-positive bacteria for halloysite samples. Bacteriocins were intercalated into the interlayer space of montmorillonites as deduced from the increase of the basal spacing measured by X-ray diffraction (XRD) assay. Infrared spectroscopy suggested non-electrostatic interactions, such as hydrogen bonding between siloxane groups from clays and peptide molecules. Transmission electron microscopy did not show any alteration in morphologies after adsorption of antimicrobial peptides on bentonite and halloysite. These results indicate that nanoclays, especially halloysite, are suitable nanocarriers for nisin and pediocin adsorption.



## 1. Introduction

There has been great interest in the use of antimicrobial peptides, such as bacteriocins, in food preservation, health care and pharmaceutical applications. These molecules differ from traditional antibiotics and are less likely to cause pathogen resistance (Brandelli, 2012; Ibarguren, Audisio, Torres, & Apella, 2010). Bacteriocins are natural occurring compounds with a wide range of antimicrobial activities and proteinaceous nature, which implies a putative degradation in the gastrointestinal tract of humans and animals (Cleveland, Montville, Nes, & Chikindas, 2001). In terms of food safety, the bacteriocins from lactic acid bacteria (LAB) have received much attention due to their generally recognized as safe (GRAS) status and potential use as natural preservatives (Cotter, Hill, & Ross, 2005; Papagianni & Anastasiadou, 2009).

The most studied LAB bacteriocin, nisin, is a polypeptide of 34 amino acids produced by *Lactococcus lactis* strains. This bacteriocin contains lanthionine and methyllanthionine residues, a molecular mass of 3500 Da, and displays a wide spectrum of activity against Gram-positive bacteria and on spores of Bacilli and Clostridia (Arauz, Jozala, Mazzola, & Penna, 2009). Unlike nisin, pediocin AcH (same of PA-1) has 44 amino acids (molecular mass of 4629 Da), is produced by *Pediococcus acidilactici* and is commercially exploited as a bacteriocin-containing fermentate powder. Pediocin is part of a group of bacteriocins belonging to the class IIa, characterized as "antilisterial" bacteriocins (Papagianni & Anastasiadou, 2009).

These bacteriocins are commonly incorporated into food by direct addition for controlling pathogenic bacteria. However, some loss of antimicrobial activity can occur due to proteolytic degradation or potential interaction with food components (Cleveland et al., 2001; Malheiros, Daroit, & Brandelli, 2010). In this sense, nanostructures may represent an interesting alternative as bacteriocin carriers, not only for food but also for medical applications, improving their stability and efficacy (Brandelli, 2012).

Nanoclays or layered silicates typically have a stacked arrangement of silicate layers with a nanometric thickness. They have been used for remediation of environmental contaminants, delivery of drugs and various active molecules, and to enhance polymer mechanical and barrier properties in packaging films (Azeredo, 2013; Parolo et al., 2010; Rawtani & Agrawal, 2012). Furthermore, mineral clays may allow a controlled release of antimicrobials and are considered as safe food additives according to FDA (US Food and Drug Administration) and EFSA (European Food Safety Authority) (Ibarguren et al., 2014). Their basic building blocks are tetrahedral sheets in which silicon is surrounded by four oxygen atoms, and octahedral sheets in which a metal-like aluminum is surrounded by eight oxygen atoms. Montmorillonite

* Corresponding author at: ICTA-UFRGS, Av. Bento Gonçalves 9500, 91501-970 Porto Alegre, RS, Brazil.
*E-mail address:* abrand@ufrgs.br (A. Brandelli).

http://dx.doi.org/10.1016/j.foodchem.2015.04.136
0308-8146/

(MMT) is a member of the smectite group, belonging to the structural family of the 2:1 phyllosilicates. It is one of the most widely used natural clays with a general formula of $M_x(Al_{4-x}Mg_x)Si_8O_{20}(OH)_4$, where M is a monovalent cation and $x$ is the degree of isomorphous substitution (between 0.5 and 1.3) (Azeredo, 2013; Pavlidou & Papaspyrides, 2008). Halloysite (HNT) is an important member of the kaolin group of clay minerals, with a composition of $Al_2Si_2O_5(OH)_4 \cdot H_2O$ with 1:1 layer (Rawtani & Agrawal, 2012). Studies on the use of nanoclays as carriers for bacteriocins are restricted to nisin onto raw montmorillonite (Ibarguren et al., 2014).

The aim of this study was to evaluate and compare the interaction of the bacteriocins nisin and pediocin with three different types of clay nanoparticles: montmorillonite modified with octadecylamine, unmodified montmorilonite (hydrophilic bentonite) and halloysite.

## 2. Materials and methods

### 2.1. Materials

Commercial nisin (Nisaplin®) was provided by Danisco Brasil Ltda. According to the manufacturer, the formulation contains NaCl and denatured milk solids as fillers, and 2.5% pure nisin. Stock solution of nisin was prepared by dissolving Nisaplin® in 10 mM of sodium phosphate monobasic monohydrate (pH 5.0). This suspension was then centrifuged (5000*g* for 10 min) to remove insoluble whey proteins from the preparation. Different working solutions of nisin were prepared by dilution of the stock nisin solution previously filter-sterilized through 0.22 μm membranes (Millipore). Nisin solutions were stored at 4 °C until their use.

Pediocin (ALTA™ 2345) was provided by Kerry Ingredients & Flavours, USA. To reach the desired concentrations, pediocin was diluted with 10 mM sodium phosphate buffer (pH 7.0). Until their use, pediocin solutions were also stored at 4 °C.

Three commercial nanoclays from Sigma–Aldrich were used: hydrophilic bentonite (Nanomer® PGV), montmorillonite (MMT) surface modified with 25–30 wt% octadecylamine (Nanomer® I.30E) and a unmodified tubular clay, halloysite (HNT).

### 2.2. Nisin adsorption on nanoclays

Adsorption assays were carried out by adding 1 ml nisin solution (0.1, 0.25, 0.5, 1.0, 1.25, 1.5, 2.0 and 2.5 mg $ml^{-1}$) or 1 ml pediocin solution (10, 50, 100, 150, 200 and 300 mg $ml^{-1}$) to 10 mg of each nanoclay. These bacteriocin-nanoclay systems were maintained during 1 h at 25 °C and 80 rpm. Preliminary experiments showed that this time was enough to reach equilibrium. After that, aliquots of supernatants were recovered by centrifugation (5000*g* for 5 min at 25 °C) and residual antimicrobial activity was determined. The pellets obtained after centrifugation (nanoclays adsorbed with bacteriocin) were washed twice with 10 mM phosphate buffer solution (pH 7.0), redispersed in the same buffer and also assessed for antimicrobial activity. Additionally, nisin and pediocin solutions at different concentrations were evaluated for initial antimicrobial activity.

### 2.3. Antimicrobial activity evaluation

The antimicrobial activity was detected by an agar diffusion assay. An aliquot of 10 μl of bacteriocin solutions, supernatants after adsorption and adsorbed nanoclays were applied on BHI agar plates previously inoculated with a swab submerged in the indicator strain (*Listeria monocytogenes* ATCC 7644) suspension, which corresponded to a 0.5 McFarland turbidity standard solution (approximately $10^7$ CFU $ml^{-1}$). Plates were chilled at 4 °C for 24 h to favor bacteriocin migration before incubation at 37 °C for 24 h. The reciprocal value of the highest dilution that produced an inhibition zone was taken as the activity unit (AU) per ml (Motta & Brandelli, 2002). A percentage of adsorbed bacteriocin activity was calculated as follows: [(initial activity of bacteriocin solution − residual activity at supernatant after adsorption)/initial activity of bacteriocin solution] × 100.

The bacteriocin-adsorbed nanoclays were also tested using 1% (w/v) skim milk agar previously inoculated with a swab submerged in suspensions of the Gram-positive bacteria *Bacillus cereus* ATCC 9634, *Clostridium perfringens* ATCC 3624, *Staphylococcus aureus* ATCC 25923 and *L. monocytogenes* ATCC 7644.

### 2.4. Characterization of samples after adsorption

After exposure to bacteriocin solutions at the saturation level, the nanoclays were washed as described in the Section 2.2. The samples were freeze-dried and submitted to X-ray diffraction (XRD), transmission electron microscopy (TEM) and infrared spectroscopy analyses. Nisaplin, ALTA™ 2345 and commercial nanoclay samples were also analyzed as controls.

XRD measurements were performed using a Siemens D-500 diffractometer (Siemens, Karlsruhe, Germany). Samples were scanned in the reflection mode using an incident X-ray of Cu Kα ($\lambda$ = 1.54 Å), at a step width of 0.05°$s^{-1}$ from $2\theta$ = 2–45°. The dispersion of the layers in the nanocomposites, as well as the basal spacing of the clays, were estimated from the (001) diffraction.

Fourier transform infrared (FTIR) spectra were measured using a Varian 640-IR spectrometer (Varian Inc., Palo Alto, CA, USA) in attenuated total reflectance (ATR) mode with a diamond crystal. The scans were collected between 400 and 4000 $cm^{-1}$.

The morphology of bentonite and halloysite samples with or without adsorbed bacteriocins was examined by TEM using a JEM-1200 Ex II electron microscope (Jeol, Tokyo, Japan) operated at an accelerating voltage of 80 kV.

### 2.5. Statistical analysis

All experiments were performed in triplicate. Results were subjected to variance analysis (ANOVA) and means were compared by the Tukey test at a level of 95% of significance ($P < 0.05$), using the SAS 9.3 software (SAS Institute, Cary, NC, USA).

## 3. Results

### 3.1. Nisin and pediocin adsorption on nanoclays

The bacteriocins nisin and pediocin adsorbed onto the three nanoclays tested, regardless of the different characteristics of these nanoparticles. However, the rate of adsorption varied substantially. The adsorption of nisin was higher onto hydrophilic bentonite (Table 1), since no residual antimicrobial activity was detected in the supernatants exposed to this nanoclay until the concentration of 2.0 mg/ml nisin solution. For MMT modified with octadecylamine, nisin solutions with concentrations greater than 1.25 mg/ml led to saturation of the clay surface, evidenced by increasing values of residual antimicrobial activity from this point (Table 1). Halloysite presented the lowest adsorption potential comparing to the other clays, because lower percentages of adsorbed nisin activity were obtained when it was exposed to increasing concentrations of nisin solutions (Table 1).

Pediocin exhibited a similar behavior when adsorbed onto nanoclays (Table 2). At the concentration of 300 mg/ml pediocin,

**Table 1**
Residual antimicrobial activity and adsorbed nisin activity after nanoclays exposure to bacteriocin solutions.

| Concentration of nisin solutions (mg/ml) | Initial antimicrobial activity of nisin solutions (AU/ml) | Residual antimicrobial activity (AU/ml); adsorbed nisin activity (%)[a] | | |
|---|---|---|---|---|
| | | Hydrophilic bentonite | Montmorillonite modified with octadecylamine | Halloysite |
| 0.1 | 400 | 0; (100) | 0; (100) | 0; (100) |
| 0.25 | 800 | 0; (100) | 0; (100) | 0; (100) |
| 0.5 | 1600 | 0; (100) | 0; (100) | 0; (100) |
| 1.0 | 4800 | 0; (100) | 0; (100) | 100; (97.9) |
| 1.25 | 6400 | 0; (100) | 0; (100) | 400; (93.7) |
| 1.5 | 7200 | 0; (100) | 100; (98.6) | 800; (88.9) |
| 2.0 | 9600 | 0; (100) | 200; (97.9) | 1600; (83.3) |
| 2.5 | 12,800 | 100; (99.2) | 400; (96.9) | 3200; (75.0) |

[a] Values are the average of three independent experiments.

**Table 2**
Residual antimicrobial activity and adsorbed pediocin activity after nanoclays exposure to bacteriocin solutions.

| Concentration of pediocin solutions (mg/ml) | Initial antimicrobial activity of pediocin solutions (AU/ml) | Residual antimicrobial activity (AU/ml); adsorbed pediocin activity (%)[a] | | |
|---|---|---|---|---|
| | | Hydrophilic bentonite | Montmorillonite modified with octadecylamine | Halloysite |
| 10 | 100 | 0; (100) | 0; (100) | 0; (100) |
| 50 | 800 | 0; (100) | 0; (100) | 0; (100) |
| 100 | 1600 | 0; (100) | 0; (100) | 0; (100) |
| 150 | 6400 | 0; (100) | 0; (100) | 200; (96.9) |
| 200 | 12,800 | 0; (100) | 0; (100) | 400; (96.9) |
| 300 | 25,600 | 100; (99.6) | 100; (99.6) | 800; (96.9) |

[a] Values are the average of three independent experiments.

the surfaces of bentonite and MMT modified with octadecylamine became saturated. Halloysite, however, adsorbed no more pediocin above the concentration of 150 mg/ml, as shown in Table 2.

Once adsorbed on nanoclays, nisin maintained its antimicrobial activity and inhibition zones were visible when aliquots of nisin-adsorbed nanoclays (suspended in buffer after washing) were applied on BHI agar plates inoculated with *L. monocytogenes* (Fig. 1). Higher inhibition zones were obtained for halloysite samples adsorbed with nisin (Fig. 1), which could be attributed to higher desorption of nisin when in contact with the agar medium. In contrast, after adsorption of pediocin on nanoclays, halos were only visualized for halloysite-adsorbed samples on BHI agar plates (data not shown). Nanoclays without nisin and pediocin did not exhibit any antimicrobial activity as expected.

When skimmed milk agar was used as a food simulant, the same behavior occurred. Nisin adsorbed on halloysite exhibited higher inhibition zones comparing to other clays, not only against *L. monocytogenes*, but also against the other Gram-positive bacteria tested, *C. perfringens* and *S. aureus* (data not shown). However, *B. cereus* was not significantly inhibited by any of the clays adsorbed with nisin. In relation to pediocin-adsorbed nanoclays, halos were only observed for halloysite samples against *L. monocytogenes* and *C. perfringens*. Pediocin adsorbed on halloysite demonstrated higher desorption on skimmed milk agar than on BHI agar plates, evidenced by the diameter of inhibition zones (Table S1).

### 3.2. Characterization of bacteriocin-adsorbed nanoclays

The XRD analysis was performed for nanoclay characterization. In relation to clay powders, XRD patterns display the level of intercalation by the measurement of interlayer spacing ($d_{001}$) from the $2\theta$ position of the clay (001) diffraction peak using Bragg's law. The XRD spectra for bacteriocin-adsorbed nanoclays are depicted in Fig. 2.

In this work, bentonite showed a basal reflection peak ($d_{001}$) at $2\theta = 6.5°$, accounting for a 1.37 nm interlayer distance (Fig. 2a). The position of this clay diffraction peak changed to $2\theta = 5.8°$ after nisin adsorption, increasing the interlayer spacing of the clay to 1.53 nm with the presence of the antimicrobial agent. A similar behavior was observed after pediocin adsorption with an increasing of interlayer space of the bentonite to 1.41 nm (Fig. 2a).

Fig. 2b shows MMT modified with octadecylamine with a basal reflection peak ($d_{001}$) at $2\theta = 4.2°$ corresponding to 2.12 nm of interlayer spacing, which was altered to 2.26 nm for nisin-adsorbed nanoclay ($2\theta = 3.9°$). However, after pediocin adsorption, two ($d_{001}$) diffraction lines appeared: one at 4.8° corresponding to 1.84 nm and a second line at lower angles (3.4°), indicating a modification of the interlayer space distance due to an intercalation of the pediocin molecules in the solid matrix (Fig. 2b).

HNT is a non-swelling clay and dispersion cannot be accessed by XRD. It is possible to observe a diffraction peak at $2\theta = 11.7°$, corresponding to a basal spacing of 0.75 nm (Fig. 2c). After nisin and pediocin adsorption, the diffraction peak of HNT internal channel was not shifted, confirming that the channel structure of the primary particles remained unchanged.

Nisin powder was also analyzed by XDR and a remarkable peak at 31.7–31.8° was detected (Fig. 2d). This corresponds to the characteristic diffraction pattern of sodium chloride (NaCl), a component of Nisaplin® (Bastarrachea et al., 2010). Nevertheless, this band is not present in adsorbed-nanoclays samples. In contrast, pediocin powder did not exhibit peaks when analyzed by XRD, indicating no crystalline substances are present in its formulation (data not shown).

FTIR spectroscopy is a sensitive technique largely used to reveal adsorption of surfactants or pollutants onto nanoclays. In this

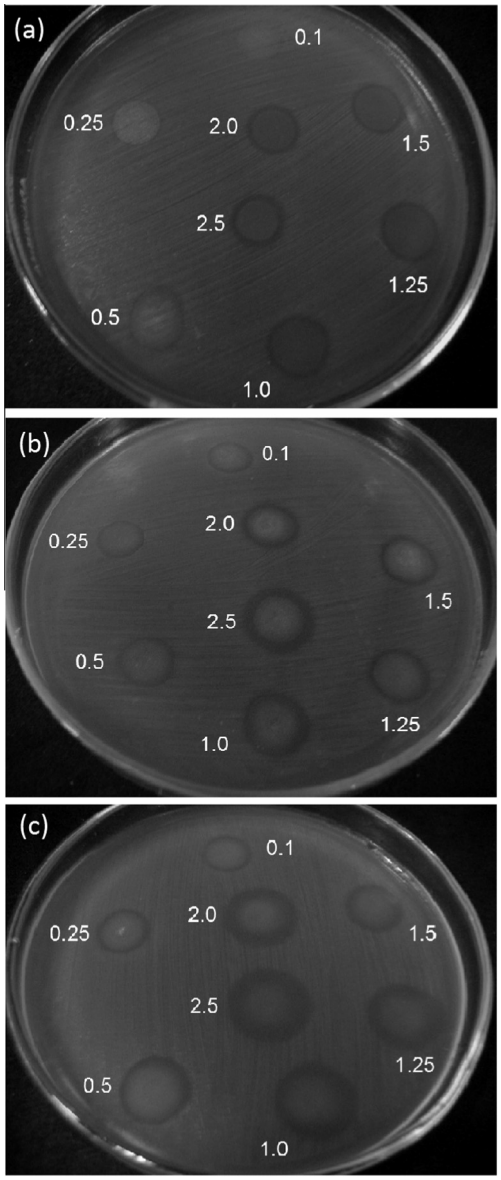


**Fig. 1.** Antimicrobial activity of nanoclays (a) bentonite, (b) MMT modified with octadecylamine, (c) HNT after nisin adsorption. Values indicate different concentrations of nisin adsorbed to nanoclays (0.1–2.5 mg/ml).

work, FTIR was used to explore the molecular environment of the nanoclays after interaction with nisin and pediocin (Fig. 3). The common features in the FTIR spectra of nanoclays were the presence of characteristic bands around 3622 $cm^{-1}$ attributed to the –OH stretching vibration of structural hydroxyl groups, 1640 $cm^{-1}$ related to the –OH deformation of water and 1028 $cm^{-1}$ assigned to siloxane (Si–O) stretching vibration. The band around 910 $cm^{-1}$ was assigned to isolated Si–O groups and it was more intense in HNT than in the other clays. A shoulder around 1100 $cm^{-1}$ observed in bentonite and HNT is attributed to Si–O deformation.

In particular, bentonite showed a band around 3420 $cm^{-1}$ related to the –OH stretching of water, indicating an Si–OH interaction with physisorbed water (Fig. 3a). This band appears broad and weaker in the samples with nisin and pediocin. Other bands due to the presence of octadecylamine are visible in Fig. 3b: 2920 $cm^{-1}$, related to C–H asymmetric stretchings of $CH_2$ or $CH_3$; 2850 $cm^{-1}$, corresponding to C–H symmetric stretchings of $CH_2$ or $CH_3$; and 1465 $cm^{-1}$ that is attributed to $CH_2$ scissoring (Chuayjuljit, Thongraar, & Saravari, 2008). On the other hand, HNT presents a band at 3694 $cm^{-1}$ (Fig. 3c), indicating the presence of silanol groups. HNT spectra of samples adsorbed with nisin and pediocin showed a minor alteration of the siloxane band doublets comparing to HNT alone (Fig. 3c, inset).

The commercial nisin preparation, Nisaplin®, contains NaCl, carbohydrate and moisture in the formulation. In this context, the major bands were obtained at 3420 and 1634 $cm^{-1}$ (Fig. 3d). In the same way, pediocin formulation shows bands at 3299 and 1585 $cm^{-1}$ (Fig. 3d). Absorption in this first area indicates stretching of the O–H and N–H bonds and the spectra in the region of 1720–1580 $cm^{-1}$ are attributed to the amide bands (Kong & Yu, 2007). The pediocin spectrum presented another intense band at 1024 $cm^{-1}$ corresponding to C–N stretching.

The morphology of MMT and HNT is illustrated in Fig. 4. MMT is a 2-to-1 layered smectite clay mineral with a platy structure. Individual platelet thicknesses are just one nanometer, but surface dimensions are generally 300 to more than 600 nm, resulting in an unusually high aspect ratio (Fig. 4a). In contrast, HNT exhibits a hollow tubular structure as the dominant morphology, resembling that of carbon nanotubes and its typical dimensions are on the nanoscale (Fig. 4c). After nisin adsorption, no morphological differences were observed by TEM images (Fig. 4b and d). Similarly, the adsorption of pediocin did not alter nanoclay morphologies (data not shown).

## 4. Discussion

MMTs and HNTs are natural hydrophilic nanoparticles. However, modifications with organic compounds like surfactants by ion exchange reactions are usually common in order to improve the compatibility of clays with polymers for their application in nanocomposites (Azeredo, 2013). For comparison, this study also used the MMT modified with octadecylamine that presents a hydrophobic characteristic. In this sense, results revelaed that nisin and pediocin interact with both surface types, regardless of polarity. Bower, McGuire, and Daeschel (1995a) also showed that nisin could adsorb onto silica surfaces with low and high hydrophobicity. On the other hand, Karam, Jama, Mamede et al. (2013) detected lower amounts of nisin on hydrophobic surfaces *versus* the hydrophilic ones.

After adsorption on the three nanoclays, nisin maintained its antimicrobial activity against *L. monocytogenes*. When applied on skimmed milk agar, nisin-adsorbed clays also inhibited *C. perfringes* and *S. aureus*. These results are consistent with previous investigations, which show that nisin adsorbed on silica surfaces retains its biological activity (Bower et al., 1995a; Wan, Gordon, Hickey, Mawson, & Coventry, 1996).

HNT exhibited the lowest capacity of adsorbing nisin and pediocin, but demonstrated the largest inhibition zones against the indicator bacteria after nisin adsorption, and it was the only nanoclay that exhibits antimicrobial activity after pediocin adsorption. Since more discrete or absence inhibition zones were obtained for bentonite and MMT-modified with octadecylamine samples, these clays may have more tightly bound or inactivated nisin and pediocin as compared to HNT.

When adsorbed on surfaces, peptides may suffer structural rearrangement and adopt different orientation and interactions (Henry, Dupont-Gillain, & Bertrand, 2003). Such conformational changes can significantly affect the antimicrobial activity and the performance of the adsorbed-material. Dawson, Harmon, Sotthibandhu, and Han (2005) reported that adsorption of nisin onto surfaces can alter the peptide conformation and result in formation of nisin multi-layers and dimers, which can reduce its

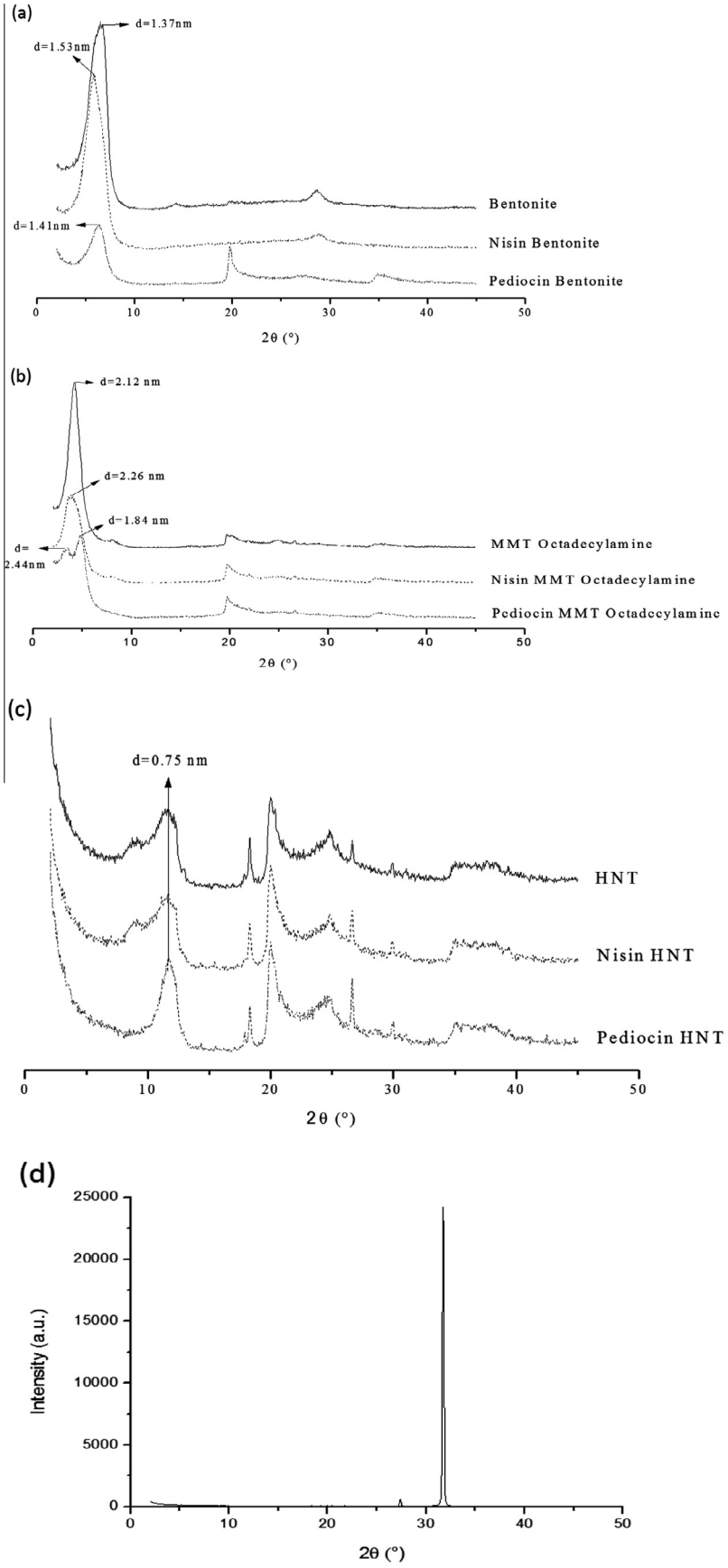


**Fig. 2.** XRD patterns of (a) bentonite, (b) MMT modified with octadecylamine, (c) HNT, before (solid line) and after nisin or pediocin adsorption(dotted lines). (d) XDR pattern of nisin preparation.

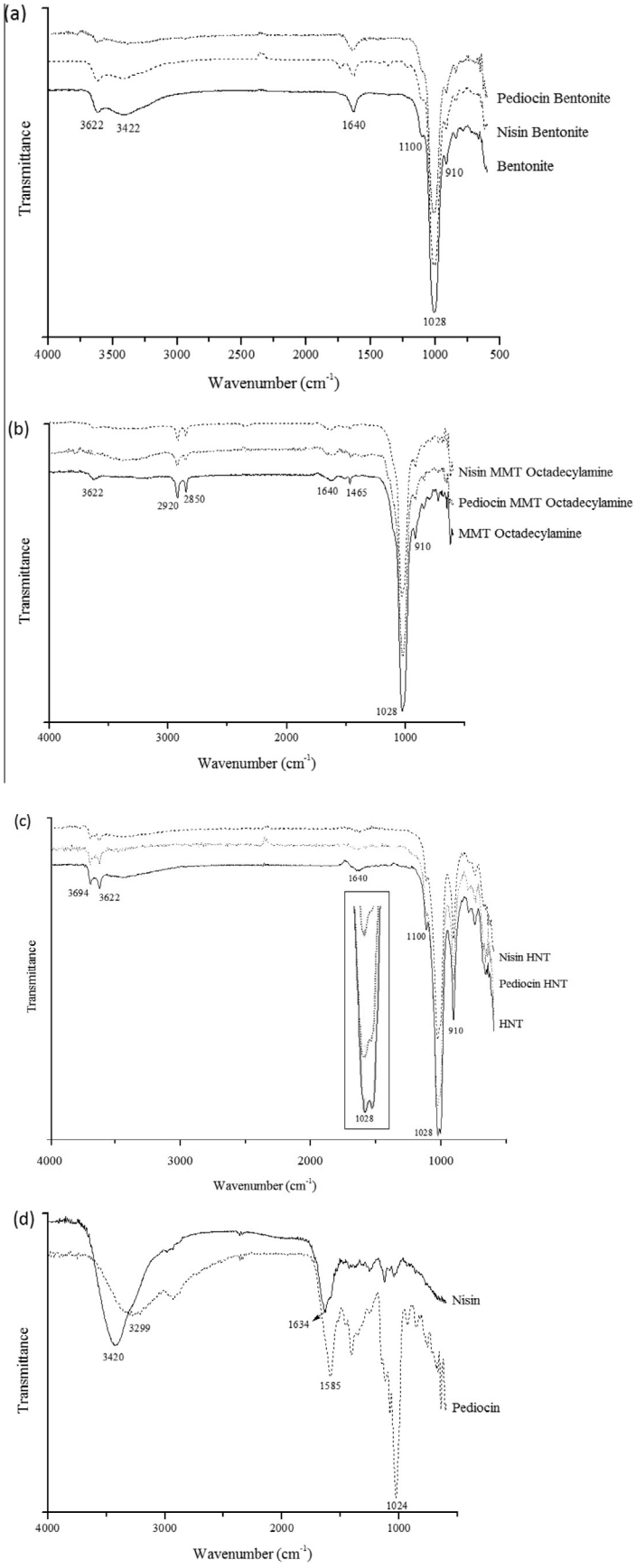


**Fig. 3.** FTIR spectra of (a) bentonite, (b) MMT modified with octadecylamine, (c) HNT, before (solid line) and after nisin or pediocin adsorption (dotted lines); inset: zoom of the peak doublet of siloxane at 1028 $cm^{-1}$. (d) FTIR spectra of nisin and pediocin.

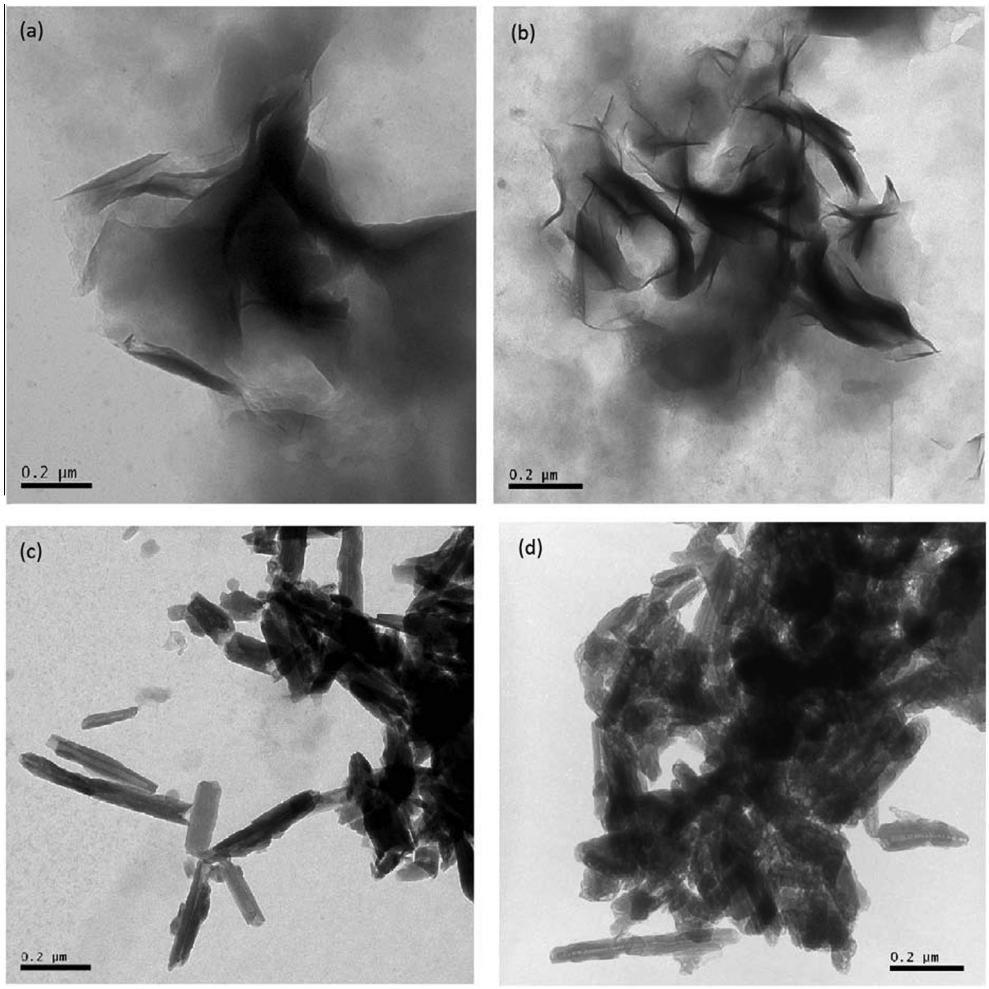


**Fig. 4.** TEM micrographs of (a) bentonite and (b) nisin-adsorbed bentonite, showing typical platelet structure; (c) HNT and (d) nisin-adsorbed HNT, showing a characteristic hollow tubular structure.

biological activity. Bower et al. (1995a) found that nisin adsorbed in small amounts on low-hydrophobic surfaces, but these samples displayed more antimicrobial activity than higher-hydrophobicity surfaces, similar to results obtained for HNT surface in the present study.

Additionally, Yu et al. (2013) reported that different clay minerals have different adsorption sites. The adsorption sites on kaolinites like HNT are only on the external surface due to their non-expanding layers. On the other hand, smectites, such as MMTs, are expanding layer silicates and thus have extensive internal and external surfaces. It is probable that nisin and pediocin adsorbed only on the external surface of HNT, making them available or freely desorbed from the HNT when compared to MMTs. These findings are in agreement with previously reported works (Karam, Jama, Nuns et al., 2013; Szabó et al., 2008).

While the bactericidal mechanisms of adsorbed nisin and pediocin have not been determined, it may require the release of these bacteriocins from the adsorbed clay surface to promote damage to the cell membrane. Nisin has been consistently shown to kill Gram-positive bacteria and the mechanism of its activity in solution involves a multi-step process that destabilizes the phospholipid bilayer of the cell and creates transient pores (Bonev, Chan, Bycroft, Roberts, & Watts, 2000; Cotter et al., 2005). According to Lante, Crapisi, Pasini, and Scalabrini (1994), when nisin cannot be desorbed from an immobilization surface, it is unavailable to adhere and hence to inhibit microbial cells. Bower, McGuire, and Daeschel (1995b) reported greater nisin activities for surfaces of lower hydrophobicity and supported a hypothesis that nisin adsorbed to hydrophilic surfaces were more freely available to enter the susceptible microorganism and begin its multi-molecular assembly within the bacterial membrane. Whereas, pediocin causes destabilization of membrane functions including loss of intracellular $K^+$, entrance of carbohydrates from the medium inside the cells and cell lysis of some strains (Papagianni & Anastasiadou, 2009).

XRD technique uses the scattered intensity of an X-ray beam on the sample, to reveal information about the crystallographic structure, chemical composition and physical properties of the material studied (Espitia et al., 2012). The hydrophilic bentonite clay shows a typical basal reflection peak ($d_{001}$) at $2\theta = 6.5°$, which is closely related with the 6.6° value described in the literature (Konwar & Karak, 2011). A slight modification in interlayer spacing of the hydrophilic MMT verified in XRD patterns may suggest intercalation of nisin and pediocin molecules, or a part of them, between bentonite layers. These results are in agreement with Ibarguren et al. (2014) who reported that nisin adsorbed on raw montomorillonite probably by "frustrated intercalation", suggesting that the cationic portions of the peptide molecule interacted with the clay mineral structure.

In relation to MMT modified with octadecylamine, adsorbed-nisin also increased the interlayer spacing, while the pediocin-adsorbed sample revealed an additional peak in the XRD spectrum.

Parolo et al. (2010) found intercalation of tetracycline after adsorption on MMTs by an extra reflection peak, coexisting two basal spacing that indicates a stacking of the nanoclay layers containing the antibiotic in the interlayer. The diffraction peak at $2\theta = 11.7°$, corresponding to a basal spacing of 0.75 nm, confirmed the tubular structure at the nanoscale of halloysite (Joussein et al., 2005).

The results of XRD may also provide information on the structural configuration of the molecule intercalated, including lateral monolayer, lateral bilayer, paraffin monolayer, paraffin bilayer and pseudo trilayer (Park, Ayoko, & Frost, 2011). However, in our case, XDR did not provide any more detailed information about the local conformation and phase state of the intercalated bacteriocins.

Electron microscopy analysis showed that bacteriocin adsorption caused no morphological modifications of nanoclays. A typical layered clay particle was observed for bentonite, where hundreds or thousands of layers are stacked together with van der Waals forces to form clay particles (Hashemifard, Ismail, & Matsuura, 2011; Pavlidou & Papaspyrides, 2008). HNT exhibited a characteristic hollow tubular structure, and its typical dimensions are in the nanoscale: 10–50 nm in outer membrane, 5–20 nm in inner diameter with 2–40 nm in length (Joussein et al., 2005; Rawtani & Agrawal, 2012).

Adsorption and binding of peptide molecules by nanoclays involve a variety of physical and chemical interactions, such as cation exchange, electrostatic interactions, hydrophobic affinity, hydrogen bonding and van der Waals forces (Yu et al., 2013). Electrostatic attractions may also play an important role in the interaction of organic substrates with MMT (Park et al., 2011; Parolo et al., 2010; Servagent-Noinville, Revault, Quiquampoix, & Baron, 2000). Nisin has a net positive charge of +5 and likely interacts with the negatively charged interface of lipid model membranes (El Jastimi, Edwards, & Lafleur, 1999). Adsorption of nisin to hydrophilic surfaces by electrostatic interactions was previously cited (Bower et al., 1995a). In the same way, pediocin contains positively charged residues, mostly located in the hydrophilic N-terminal region (Papagianni & Anastasiadou, 2009). Nisin consists of 34 amino acids including three lysine and two histidine residues. Also, pediocin contains Lys11 and His12 that are part of the cationic patch in the N-terminal β-sheet-like region of the molecule. Then, the protonation of these residual amino groups could favor electrostatic interactions between nisin and pediocin molecules and negatively-charged surfaces of the clay minerals (Ibarguren et al., 2014; Papagianni & Anastasiadou, 2009).

In addition to electrostatic forces, clay minerals are capable of binding peptide molecules since the octahedral surface and exchangeable cations in the interlayer space have a hydrophilic character, while the tetrahedral surface with hydroxyl groups and uncharged regions between charge sites present a partial hydrophobic character (Servagent-Noinville et al., 2000; Yu et al., 2013). The hydrophilic portion of the clay surface can interact with the polar amino acids, whereas hydrophobic interactions can occur between the siloxane surface of the clay mineral and non-polar amino acid side chains of the peptide (Yu et al., 2013). Nisin adsorption to silanized silica surfaces showed a higher adsorbed mass that was consistently recorded on the hydrophilic relative to the hydrophobic surface. At the hydrophobic surface, the hydrophobic domain may be oriented toward the surface, with the hydrophilic domain having less contact. Each peptide molecule is depicted as occupying a larger area on the hydrophobic surface relative to a hydrophilic one, as the amphiphilic domain is larger than the positively-charged domain (Lakamraju, McGuire, & Daeschel, 1996).

Non-electrostatic interactions, for example hydrogen bonding and van der Waals force, have been proved to be important in the adsorption mechanisms between organic species and MMTs (Parolo et al., 2010). Also, the HNT surface is composed of siloxane and has a few hydroxyl groups, which indicates that HNT possesses a potential for hydrogen bonding (Du, Guo, Lei, Liu, & Jia, 2008). The HNT spectrum shows a band at 3694 $cm^{-1}$, assigned to the presence of silanol groups that are also able to form hydrogen bonds (Ibarguren et al., 2010; Mellouk, Belhakem, Marouf-Khelifa, Schott, & Khelifa, 2011). The samples analyzed in this study showed typical assignments of clays (Du et al., 2008), and no additional bands in FTIR spectra were observed after nisin and pediocin adsorption on nanoclays. This result could be explained by the small quantity of nisin and pediocin in relation to the quantity of nanoclays used during adsorption studies. The adsorbed amount is affected by various factors, such as peptide properties (size, structure stability, amino acid composition, 3-D conformation), the solid substrate surface characteristics and environmental conditions (Van der Veen, Norde, & Stuart, 2004). However, the intensity of Si–O bands at 1028 $cm^{-1}$ was weaker in samples with bacteriocins, which indicate a possible interaction between the peptide with the nanoclays by the formation of hydrogen bonds. In the case of HNT, samples adsorbed with nisin and pediocin showed an alteration of the siloxane bands comparing to HNT alone, reflecting that non-electrostatic interactions occurred after adsorption.

## 5. Conclusions

Nisin and pediocin were able to adsorb on bentonite, MMT modified with octadecylamine and HNT. XRD analyses provide evidence on the intercalation of the peptide molecules on silicate layers. Non-electrostatic interactions were inferred by FTIR analysis after bacteriocin adsorption on nanoclays. Meanwhile, the antimicrobial activity detected using BHI and skimmed milk agar plates was better when halloysite nanotubes were used as a support agent. Therefore, halloysite adsorbed with nisin or pediocin proved to be a promising strategy as antimicrobial delivery systems.

## Acknowledgments

This work was supported by the Brazilian agencies CNPq and CAPES.

## Appendix A. Supplementary data

Supplementary data associated with this article can be found, in the online version, at http://dx.doi.org/10.1016/j.foodchem.2015.04.136.

## References

Arauz, L. J., Jozala, A. F., Mazzola, P. G., & Penna, T. C. V. (2009). Nisin biotechnological production and application: A review. *Trends in Food Science and Technology, 20*, 146–154.

Azeredo, H. M. C. (2013). Antimicrobial nanostructures in food packaging. *Trends in Food Science and Technology, 30*, 56–69.

Bastarrachea, L., Dhawan, S., Sablani, S. S., Mah, J., Kang, D., Zhang, J., et al. (2010). Biodegradable poly(butylene adipate-*co*-terephthalate) films incorporated with nisin: Characterization and effectiveness against *Listeria innocua*. *Journal of Food Science, 75*, 215–224.

Bonev, B. B., Chan, W. C., Bycroft, B. W., Roberts, G. C. K., & Watts, A. (2000). Interaction of the lantibiotic nisin in mixed lipid bilayer: A $^{3}$IP and $^{2}$H NMR study. *Biochemistry, 39*, 11425–11433.

Bower, C. K., McGuire, J., & Daeschel, M. A. (1995a). Suppression of *Listeria monocytogenes* colonization following adsorption of nisin onto silica surfaces. *Applied and Environmental Microbiology, 61*, 992–997.

Bower, C. K., McGuire, J., & Daeschel, M. A. (1995b). Influences on the antimicrobial activity of surface-adsorbed nisin. *Journal of Industrial Microbiology, 15*, 227–233.

Brandelli, A. (2012). Nanostructures as promising tools for delivery of antimicrobial peptides. *Mini-Reviews in Medicinal Chemistry, 12*, 731–741.

Chuayjuljit, S., Thongraar, R., & Saravari, O. (2008). Preparation and properties of PVC/EVA/organomodified montmorillonite nanocomposites. *Journal of Reinforced Plastics and Composites, 27*, 431–437.

Cleveland, J., Montville, T. J., Nes, I. F., & Chikindas, M. L. (2001). Bacteriocins: Safe, natural antimicrobials for food preservation. *International Journal of Food Microbiology, 71*, 1–20.

Cotter, P. D., Hill, C., & Ross, R. P. (2005). Bacteriocins: Developing innate immunity for food. *Nature Reviews in Microbiology, 3*, 777–788.

Dawson, P. L., Harmon, L., Sotthibandhu, A., & Han, I. Y. (2005). Antimicrobial activity of nisin-adsorbed silica and corn starch powders. *Food Microbiology, 22*, 93–99.

Du, M., Guo, B., Lei, Y., Liu, M., & Jia, D. (2008). Carboxylated butadiene–styrene rubber/halloysite nanotube nanocomposites: Interfacial interaction and performance. *Polymer, 49*, 4871–4876.

El Jastimi, R., Edwards, K., & Lafleur, M. (1999). Characterization of permeability and morphological perturbations induced by nisin on phosphatidylcholine membranes. *Biophysical Journal, 77*, 842–852.

Espitia, P., Soares, N. F., Coimbra, J. S. R., Andrade, N. J., Cruz, R. S., & Medeiros, E. A. A. (2012). Zinc oxide nanoparticles: Synthesis, antimicrobial activity and food packaging applications. *Food and Bioprocess Technology, 5*, 1447–1464.

Hashemifard, S. A., Ismail, A. F., & Matsuura, T. (2011). Effect of montmorillonite nano-clay fillers on PEI mixed matrix membrane for $CO_2$ removal. *Chemical Engineering Journal, 170*, 316–325.

Henry, M., Dupont-Gillain, C., & Bertrand, P. (2003). Conformation change of albumin adsorbed on polycarbonate membranes as revealed by ToF-SIMS. *Langmuir, 19*, 6271–6276.

Ibarguren, C., Audisio, M. A., Torres, E. M. F., & Apella, M. C. (2010). Silicates characterization as potential bacteriocin-carriers. *Innovative Food Science and Emerging Technologies, 11*, 197–202.

Ibarguren, C., Naranjo, P. M., Stötzel, C., Audisio, M. C., Sham, E. L., Torres, E. M. F., et al. (2014). Adsorption of nisin on raw montmorillonite. *Applied Clay Science, 90*, 88–95.

Joussein, E., Petit, S., Churchman, J., Theng, B., Righi, D., & Delvaux, B. (2005). Halloysite clay minerals – A review. *Clay Minerals, 40*, 383–426.

Karam, L., Jama, C., Mamede, A. S., Boukla, S., Dhulster, P., & Chihib, N. E. (2013). Nisin-activated hydrophobic and hydrophilic surfaces: Assessment of peptide adsorption and the antibacterial activity against some food pathogens. *Applied Microbiology and Biotechnology, 97*, 10321–10328.

Karam, L., Jama, C., Nuns, N., Mamede, A.-S., Dhulster, P., & Chihib, N.-E. (2013). Nisin adsorption on hydrophilic and hydrophobic surfaces: Evidence of its interactions and antibacterial activity. *Journal of Peptide Science, 19*, 377–385.

Kong, J., & Yu, S. (2007). Fourier transform infrared spectroscopic analysis of protein secondary structures. *Acta Biochimica et Biophysica Sinica, 39*, 549–559.

Konwar, U., & Karak, N. (2011). Hyperbranched polyether core containing vegetable oil-modified polyester and its clay nanocomposites. *Polymer Journal, 43*, 56–576.

Lakamraju, M., McGuire, J., & Daeschel, J. (1996). Nisin adsorption and exchange with selected milk proteins at silanized silica surfaces. *Journal of Colloid and Interface Science, 178*, 495–504.

Lante, A., Crapisi, A., Pasini, G., & Scalabrini, P. (1994). Nisin released from immobilization matrices as antimicrobial agent. *Biotechnology Letters, 16*, 293–298.

Malheiros, P. S., Daroit, D. J., & Brandelli, A. (2010). Food applications of liposome-encapsulated antimicrobial peptides. *Trends in Food Science and Technology, 21*, 284–292.

Mellouk, S., Belhakem, A., Marouf-Khelifa, K., Schott, J., & Khelifa, A. (2011). Cu(II) adsorption by halloysites intercalated with sodium acetate. *Journal of Colloid and Interface Science, 360*, 716–724.

Motta, A. S., & Brandelli, A. (2002). Characterization of an antimicrobial peptide produced by *Brevibacterium linens*. *Journal of Applied Microbiology, 92*, 63–67.

Papagianni, M., & Anastasiadou, S. (2009). Pediocins: The bacteriocins of Pediococci. Sources, production, properties and applications. *Microbial Cell Factories, 8*, 1–16.

Park, Y., Ayoko, G. A., & Frost, R. L. (2011). Application of organoclays for the adsorption of recalcitrant organic molecules from aqueous media. *Journal of Colloid Interface Science, 354*, 292–305.

Parolo, M. E., Avena, M. J., Pettinari, G., Zajonkovsky, I., Valles, J. M., & Baschini, M. T. (2010). Antimicrobial properties of tetracycline and minocycline-montmorillonites. *Applied Clay Science, 49*, 194–199.

Pavlidou, S., & Papaspyrides, C. D. (2008). A review on polymer-layered silicate nanocomposites. *Progress in Polymer Science, 33*, 1119–1198.

Rawtani, D., & Agrawal, Y. K. (2012). Multifarious applications of halloysite nanotubes: A review. *Reviews on Advanced Materials Science, 30*, 282–295.

Servagent-Noinville, S., Revault, M., Quiquampoix, H., & Baron, M. H. (2000). Conformational changes of bovine serum albumin induced by adsorption on different clay surfaces: FTIR analysis. *Journal of Colloid and Interface Science, 221*, 273–283.

Szabó, T., Mitea, R., Leeman, H., Premachandra, G. S., Johnston, C. T., Szekeres, M., et al. (2008). Adsorption of protamine and papain proteins on saponite. *Clays and Clay Minerals, 56*, 494–504.

Van der Veen, M., Norde, W., & Stuart, M. C. (2004). Electrostatic interactions in protein adsorption probed by comparing lysozyme and succinylated lysozyme. *Colloids and Surfaces B, 35*, 33–40.

Wan, J., Gordon, J., Hickey, M. W., Mawson, R. F., & Coventry, M. J. (1996). Adsorption of bacteriocins by ingestible silica compounds. *Journal of Applied Bacteriology, 81*, 167–173.

Yu, W. H., Li, N., Tong, D. S., Zhou, C. H., Lin, C. X., & Xu, C. U. (2013). Adsorption of proteins and nucleic acids on clay minerals and their interactions: A review. *Applied Clay Science, 80*(81), 443–452.